

Equation of State and Phase Separation in Binary Mixtures of Nonadditive Chains

Basel F. Abu-Sharkh†

Department of Chemical Engineering, King Fahd University of Petroleum & Minerals, Dhahran 31261, Saudi Arabia

Received February 11, 2000; Revised Manuscript Received September 25, 2000

ABSTRACT: Molecular dynamics simulations of equimolar mixtures of hard chains composed of equal size nonadditive segments were performed. Different degrees of polymerization, densities, and nonadditivities were used. Phase separation was investigated and visualized. The equation of state for these mixtures was investigated, and models based on the first order thermodynamic perturbation theory (TPT1) and the polymeric analogue of the Percus–Yevick approximation (PPY) were developed to predict the compressibility factor of the polymer mixtures. The TPT1 model was generally more accurate in predicting the compressibility factor than the PPY model for negative and zero nonadditivity. Phase separation between polymers interacting with positive nonadditivity was observed at high densities.

Introduction

The thermodynamics of chain molecules are of continuing interest for theoretical and industrial applications. In recent years, significant progress has been achieved toward modeling and understanding the behavior of chain fluids. Freely jointed hard sphere model chains have been the subject of many investigations because they carry the most essential features of polymeric molecules. Theoretical modeling of these systems is simpler and their simulation is less computationally expensive than real polymers. Furthermore, the hard sphere chain model can be used as a reference system for perturbation theories of more realistic polymeric systems. To understand the macroscopic properties of polymers, extensive theoretical treatments have been proposed^{1–4} and extensive simulation studies have been conducted.^{5–7} Hall and co-workers have developed theories for the hard chain fluid by extending Flory's probabilistic assumptions about lattice chains in continuous space.^{8,9} Wertheim has developed two equations of state for the hard chain fluid based on a thermodynamic perturbation theory of polymerization (TPT).^{10,11} Chiew developed an equation of state for polymers by obtaining an analytical solution to the compressibility equation of state.¹² Boublik et al. extended the scaled particle theory to flexible chain molecules.¹³

Nonadditive size interactions represent a simple model where phase separation is observed for hard sphere mixtures interacting with positive nonadditivity parameter, Δ .¹⁴ Spherical nonadditive size interaction is characterized by a cross-collision diameter σ_{ij} of the form

$$\sigma_{ij} = (1 + \Delta)(\sigma_{ii} + \sigma_{jj})/2 \geq -1 \quad (1)$$

Nonadditivity means that the distance between two unlike particles is different from the arithmetic mean of the distances σ_{ii} between like pairs. Nonadditivity is called positive or negative according to the sign of Δ . Properties of nonadditive hard sphere mixtures are significantly different from additive mixtures.¹⁴ Introduction of negative nonadditivities was found to reproduce the structure factor of real mixtures with strong

tendencies to heterocoordination.¹⁴ NAHS binary fluid mixtures phase separate at high densities when Δ is positive, into two phases, one rich in component 1 and the other rich in component 2.¹⁴ The phase separation takes place because of the higher repulsions between unlike segments when it overcomes the thermal motions that tend to mix the system.

Nonadditive interactions were used in describing liquid metals,^{15,16} protein interactions,¹⁷ and fluid–fluid phase separation at very high pressures^{18,19} where repulsive interactions dominate. The simplest molecules for which nonadditive interactions were studied are mixtures of hard spheres. Binary mixtures of equal-size components were studied by computer simulation,^{20–23} integral equations,^{14,25,26} and other analytical techniques.^{19,22,25–28} Mixtures with unequal size components were studied by computer simulation,²⁹ and expressions for the contact pair correlation functions and equations of state were developed.²⁴ In addition, a general mixture theory, which accounts for nonadditive size interactions in spherical and nonspherical molecules, has been developed.^{31,32}

There are very few studies in the literature that address nonadditive interactions in hard chains. In a study on liquid crystalline phases, nonadditive size interactions were used to form a stiff chain out of an 8-mer flexible chain.³³ In a more recent study a general method of representing chain stiffness, segment fusion, ring rigidity, and specific forces using nonadditive size interactions was suggested.³⁴ Another study investigated self-assembly in block and alternating hard chain copolymers that consist of nonadditive equal size segments.³⁵

In this study, models are developed for the equation of state of systems composed of an equimolar binary mixture of chains composed of nonadditive equal size segments based on the first order thermodynamic perturbation theory (TPT1)^{10,11} and the polymeric analogue of the Percus–Yevick approximation (PPY).¹² The models are used to predict the compressibility factors for the polymer mixtures and the results are compared to the simulation data. We also investigate phase separation in these mixtures as a function of nonadditivity, degree of polymerization, and density in order to understand the parameters that control the phase

† E-mail: sharkh@kfupm.edu.sa.

behavior in absence of attractive interactions. This study provides an alternative, computationally efficient method for studying self-assembly in polymeric mixtures and surfactants without having to use computationally expensive models with attractive potentials that are long range in nature. The advantage of this method stems from the simplicity of simulating hard chains as well as the very short range of the hard sphere potential, which limits the number of interactions of segments and hence results in more efficient simulation. This study also extends the validity of the two thermodynamic models (TPT1 and PPY) to nonadditive polymeric mixtures.

Molecular Dynamics

We consider an equimolar binary mixture of two types of chains consisting of hard sphere segments in a volume V . The chains in the mixture are of equal length and the spherical segments composing them are of equal size. The cross interaction between segments in different chains is governed by eq 1. The packing fraction of the chains is

$$\rho = \frac{\pi N}{6 V} \sum_i x_i \sigma_i^3 \quad (2)$$

where x_i is the mole fraction of spheres of type i . The total number of spheres, N , is fixed at 512. The chain model consists of m freely jointed touching hard spheres where m is equal to 4, 8, and 16. For computational convenience, the hard sphere potential between pairs of nonbonded segments (within the same molecule or within different molecules) is approximated by a truncated Lennard-Jones (LJ) potential with purely repulsive character that has the form:³⁶

$$U_{\text{HS}}(r) = 4\epsilon \left[\left(\frac{\sigma}{r} \right)^{12} - \left(\frac{\sigma}{r} \right)^6 \right] + \epsilon, \quad r < 2^{1/6}\sigma \quad (3)$$

$$= 0, \quad r > 2^{1/6}\sigma$$

where r is the distance between any pair of interacting segments. All spherical segments in the system are assigned the same values of ϵ . Interactions between segments of the same polymeric component are additive while nonadditive interactions are applied between segments of different components of the mixture.

We perform molecular dynamics simulations in a cubic box with periodic boundary conditions. We employ the DL_POLY 2.0 simulation program³⁷ in the NVT ensemble. The distances between bonded spheres are constrained using the shake algorithm. The value of ϵ/kT in eq 3 is fixed at 0.8. This value of ϵ/kT makes the parameter σ of the Lennard-Jones potential effectively equivalent to the hard sphere diameter (σ).³⁶ Our compressibility factor results compare well with Monte Carlo and discontinuous molecular dynamics results for additive hard sphere chains as shown in Figure 1.^{37,38}

Each system is started from a cubic lattice of chains randomly placed. The initial velocities are generated according to the Maxwell-Boltzmann distribution. Each system is initially relaxed by performing a simulation of 4×10^5 molecular dynamics time steps. Compressibility factor data are then collected over 1×10^5 steps. Increasing the number of time steps to 10^6 resulted in less than 0.1% change in the calculated average compressibility factor. The equation of motion is integrated

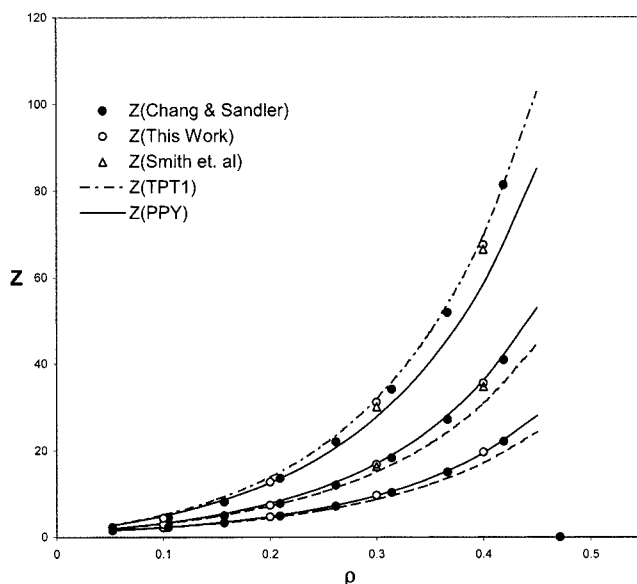


Figure 1. Comparison between the simulation data of this work, Chang and Sandler, and Smith et al. and predictions of the TPT1 and PPY models for additive hard chains.

using the Verlet algorithm as provided with the DL_POLY 2.0 program. The time step for the simulation is 0.5 fs. The simulations are carried out for four different packing fractions: $\rho = 0.1, 0.2, 0.3$, and 0.4 and five different nonadditivity ratios: $\Delta = -0.5, -0.1, 0.0, 0.05$, and 0.1 . The cutoff radius for the Verlet neighborhood list is kept constant at 2σ .

Model Development

The presence of nonadditive size interactions excludes a lattice-based model. Therefore, we seek off-lattice models that are general enough to allow nonadditive interactions between segments. In this work we base our models on the first-order perturbation theory of associating fluids (TPT1)^{10,11,40} and the PPY theory.¹² In the literature, the work done using these models was based on additive interactions. It is the objective of this work to extend the validity of these models to nonadditive chain mixtures. In general, the equation of state of m repeat unit chains can be written as

$$Z = m(Z_{\text{units}} + Z_{\text{bond}}) \quad (4)$$

where the first term between the brackets is the compressibility factor of un-bonded units, and the second term is a perturbation that accounts for the change in Z due to the presence of bonds between the units in a polymer chain. The general form of the bonding contribution, Z_{bond} for M multicomponent mixtures and heteronuclear chains containing additive hard spherical units was given by Malakhov and Brun⁴¹

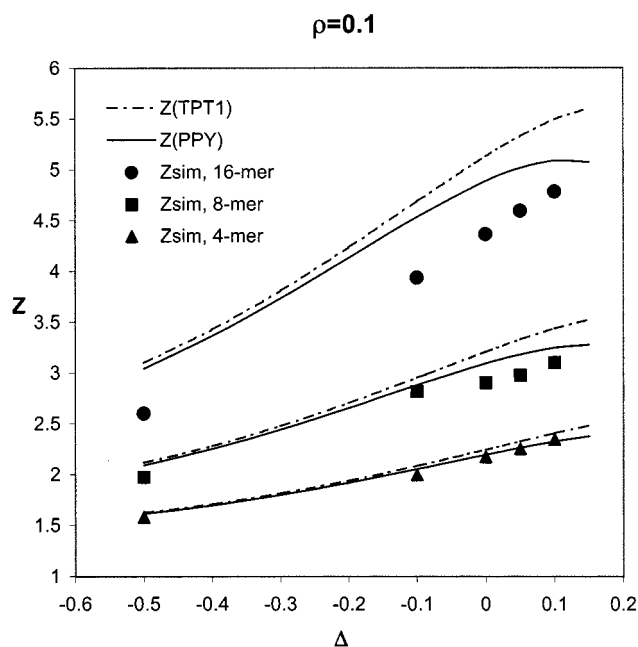
$$Z_{\text{bond}} = - \sum_{k=1}^M \sum_{s=1}^{N_k-1} \frac{\rho_{c(k)}}{\rho} \left[1 + \rho \frac{\partial(\ln g_{sk,(s+1)k})}{\partial \rho} \right] \quad \text{TPT1} \quad (5)$$

$$Z_{\text{bond}} = - \sum_{k=1}^M \sum_{s=1}^{N_k-1} \frac{\rho_{c(k)}}{\rho} g_{sk,(s+1)k} \quad \text{PPY} \quad (6)$$

where the subscript k runs over chain type and the subscript s runs over segments in each chain. In the

Table 1. Simulation and Model Compressibility Factor Data for the 16-mer, 8-mer and 4-mer Mixtures

<i>m</i>	Δ_{12}	$\rho = 0.4$			$\rho = 0.3$			$\rho = 0.2$			$\rho = 0.1$		
		Z_{sim}	$Z(\text{TPT1})$	$Z(\text{PPY})$	Z_{sim}	$Z(\text{TPT1})$	$Z(\text{PPY})$	Z_{sim}	$Z(\text{TPT1})$	$Z(\text{PPY})$	Z_{sim}	$Z(\text{TPT1})$	$Z(\text{PPY})$
16	-0.5	14.904	16.583	14.885	9.310	10.449	9.680	5.299	6.130	5.852	2.602	3.100	3.043
	-0.1	47.787	48.953	44.094	23.934	24.661	22.482	10.688	11.696	10.924	3.934	4.687	4.531
	0	69.495	69.595	58.444	31.098	31.942	27.746	12.754	13.917	12.594	4.362	5.130	4.885
	0.05	76.242	85.517	66.362	33.966	36.597	30.317	13.665	15.118	13.314	4.592	5.327	5.014
	0.1	79.493	111.034	73.994	35.445	42.411	32.414	14.468	16.353	13.820	4.782	5.490	5.086
8	-0.5	8.486	9.111	8.302	5.487	5.949	5.584	3.373	3.705	3.574	1.972	2.116	2.089
	-0.1	24.876	25.559	23.269	12.948	13.222	12.196	6.242	6.584	6.222	2.817	2.951	2.879
	0	36.088	36.157	30.889	16.743	17.025	15.047	7.321	7.778	7.156	2.903	3.205	3.091
	0.05	39.304	44.394	35.281	18.499	19.483	16.515	7.934	8.439	7.591	2.974	3.326	3.179
	0.1	41.373	57.572	39.870	19.082	22.576	17.840	8.361	9.136	7.943	3.100	3.434	3.245
4	-0.5	5.202	5.375	5.010	3.581	3.698	3.536	2.419	2.493	2.435	1.582	1.624	1.613
	-0.1	13.583	13.862	12.857	7.468	7.502	7.053	3.955	4.028	3.871	1.995	2.084	2.052
	0	19.608	19.454	17.111	9.589	9.567	8.697	4.643	4.708	4.438	2.172	2.243	2.193
	0.05	21.562	23.832	19.741	10.710	10.926	9.614	4.987	5.099	4.729	2.253	2.325	2.262
	0.1	22.431	30.840	22.808	11.100	12.658	10.553	5.336	5.527	5.005	2.343	2.406	2.324

**Figure 2.** Simulation and model compressibility factor vs nonadditivity (Δ), $\rho = 0.1$.

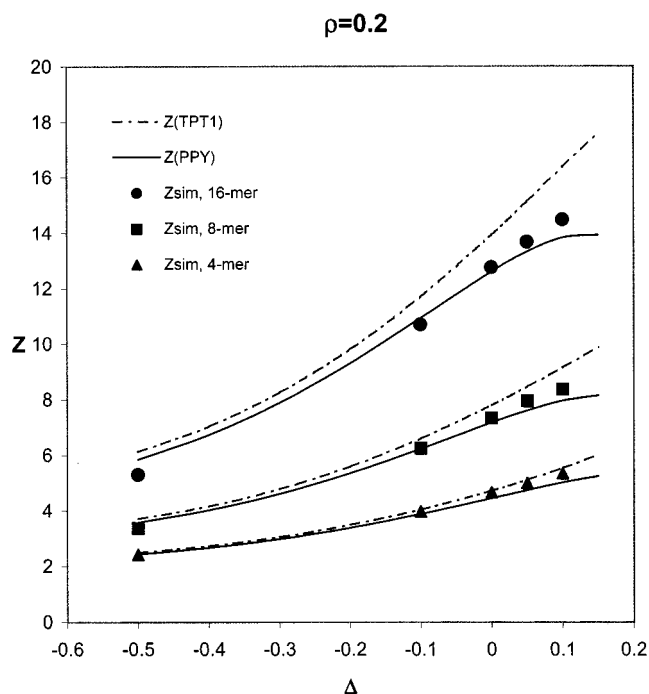
above expression N_k is the degree of polymerization, ρ is the particle density, $\rho_{c(k)}$ is the density of chains of type k , and $g_{sk,(s+1)k}$ is the contact pair correlation function between consecutive segment types in the chain. Equation 5 was derived for spherical segments interacting with additive size parameters and its validity to modeling copolymer chains composed of nonadditive segments has been verified.³⁵

In this work, we will consider an equimolar binary mixture of two types of chains. The two types of chains have the same number of segments and the segments have the same size. However, the segments of the two types of chains interact with each other nonadditively. For this polymer mixture, combining eq 4 and 5 leads to the following equation of state:

$$Z^{\text{TPT1}} = 1 + m(Z_{\text{NAHS}} - 1) - x_1(m-1) \left[\rho \frac{\partial \ln(g_{11})}{\partial \rho} \right] - x_2(m-1) \left[\rho \frac{\partial \ln(g_{22})}{\partial \rho} \right] \quad (7)$$

and combining eq 4 and 6 gives

$$Z^{\text{PPY}} = mZ_{\text{NAHS}} - x_1(m-1)g_{11} - x_2(m-1)g_{22} \quad (8)$$

**Figure 3.** Simulation and model compressibility factor vs nonadditivity (Δ), $\rho = 0.2$.

where m is the total number of segments in each chain and x_1 and x_2 are the mole fractions of components 1 and 2. We can observe that only the like pair correlation functions (g_{11} and g_{22}) appear in the bonding term of the equation.

To use eq 7 and 8, we will need expressions for the compressibility factor and the contact values of the pair correlation function of nonadditive hard sphere (NAHS) fluids. Two forms are available for these quantities.³¹ The more accurate form is complex and requires numerical integration. In this work, we will use the simpler, slightly less accurate form. The values of the like pair correlation functions at contact (g_{11} and g_{22}) that appear in eq 7 and eq 8 are obtained by replacing σ_{jj} in additive pair correlation functions g_{ii}^{add} by the quantities indicated below³¹

$$g_{ii} = \lim_{\sigma_{jj} \rightarrow (2\sigma_{ij} - \sigma_{ii})} g_{ii}^{\text{add}} \quad j \neq i \quad \sigma_{ij} \geq \sigma_{ii}/2 \quad (9)$$

$$g_{ii} = \lim_{\sigma_{jj} \rightarrow 0} g_{ii}^{\text{add}} \quad \sigma_{ij} \leq \sigma_{ii}/2 \quad (10)$$

where g_{ii}^{add} is any expression for the contact value of

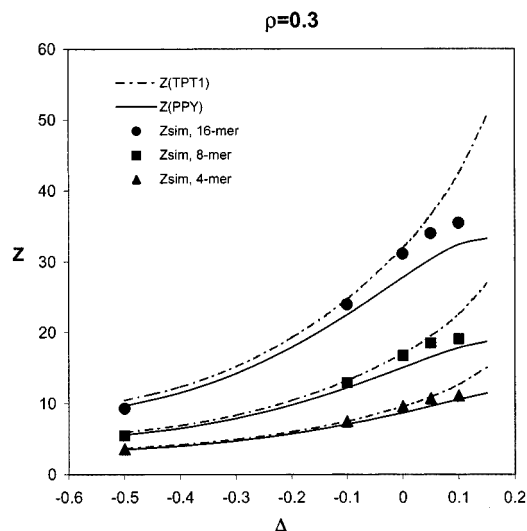


Figure 4. Simulation and model compressibility factor vs nonadditivity (Δ), $\rho = 0.3$.

the pair correlation function of additive hard spheres. Here, we use the Mansoori–Carnahan–Starling–Leland (MCSL) for g_{ii}^{add} in conjunction with the TPT1 model and the Percus–Yevick (PY) expression in conjunction with the PPY model^{41,42}

$$g_{ii}^{\text{MCSL}} = \frac{1}{1 - y_3} + \frac{3\sigma_{ii}y_2}{2(1 - y_3)^2} + \frac{y_2^2 \sigma_{ii}^2}{2(1 - y_3)^3} \quad (11)$$

$$g_{ii}^{\text{PY}} = \frac{1}{1 - y_3} + \frac{3\sigma_{ii}y_2}{2(1 - y_3)^2} \quad (12)$$

where y_2 and y_3 are given by

$$y_j = \frac{\pi}{6} \sum_{i=1}^2 \rho_i \sigma_i^j \quad (13)$$

The contact value of the unlike pair correlation function for NAHS is given by³¹

$$g_{ij} = \frac{1}{1 - y_3} + \frac{\frac{\pi}{6} \rho \sum_k x_k f_{ij,k}}{2(1 - y_3)^2} + \lambda \frac{\left(\frac{\pi}{6} \rho \sum_k x_k f_{ij,k} \right)^2}{(1 - y_3)^2} \quad (14)$$

where for binary mixtures

$$f_{ij,k} = \sigma_{kk}^3 (2\sigma_{ij} - \sigma_{kk}) / \sigma_{ij} \quad \sigma_{ij} \geq \sigma_{kk}/2 \quad (15)$$

$$f_{ij,k} = 0 \quad \sigma_{ij} \leq \sigma_{kk}/2 \quad (16)$$

$$\lambda = 1/2 \quad \text{MCSL} \quad (17)$$

$$\lambda = 3/4 \quad \text{PY} \quad (18)$$

The compressibility factor for the nonbonded spheres is obtained from the virial equation of statistical mechanics:

$$Z_{\text{NAHS}} = 1 + \frac{4\pi}{6} \rho \sum_i \sum_j x_i x_j \sigma_{ij}^3 g_{ij} \quad (19)$$

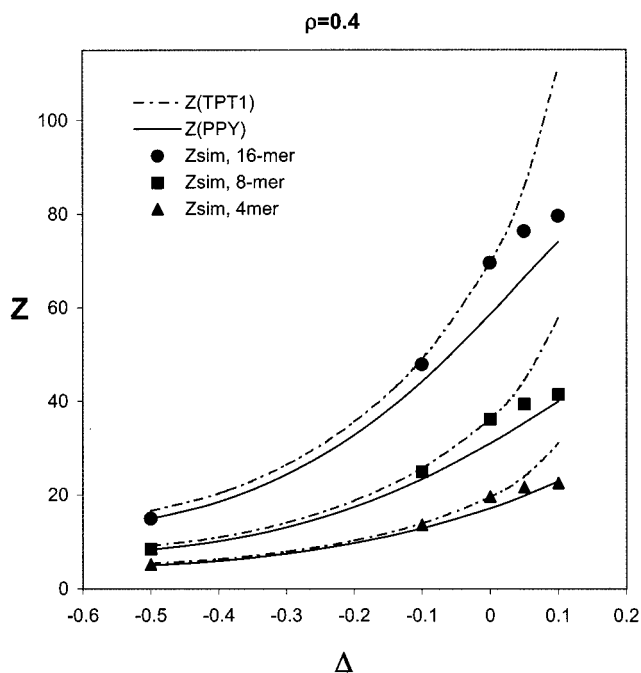


Figure 5. Simulation and model compressibility factor vs nonadditivity (Δ), $\rho = 0.4$.

The simulation and model results are presented in the following section.

Results and Discussion

The simulation and the two model values of the compressibility factors for the 4-mer, 8-mer, and 16-mer chains are shown in Table 1. To test the models presented above for nonadditive chains we compare their predictions of the compressibility factor with the simulation data in Figures 2–5, which show the compressibility factor as a function of the nonadditivity parameter (Δ) at different densities. The accuracy of the TPT1 model is higher for shorter chains and at higher densities. Large deviations are observed for the PPY model especially at higher densities. The models show higher accuracy at negative values of Δ than positive values. For positive values of (Δ), the TPT model tends to overpredict the compressibility factor as Δ increases. On the other hand, the PPY model follows the correct curvature of the compressibility factor data at positive nonadditivities as compared to the TPT1 compressibility factor data which show a monotonic increase in Z as Δ increases. This indicates that the PPY model is better in predicting the phase behavior of the mixture, as will be discussed later. At positive Δ , increasing the density leads to larger deviations in the TPT1 model from simulation data. Deviations of the models from the simulation data can be attributed to errors introduced by use of the less accurate form of the unlike pair correlation function. The higher accuracy of the TPT1 model at higher densities can be a result of its utilization of the more accurate MCSL expressions for the pair correlation functions.

To investigate the influence of nonadditivity on the phase behavior of the simulated mixture at positive Δ , the two 8-mers composing the mixture are shown in Figure 6, parts a and b, at two positive nonadditivity parameter values of $\Delta = 0.05$ and $\Delta = 0.1$ and the minimum and maximum densities 0.1 and 0.4. The upper two plots display the configuration of the first

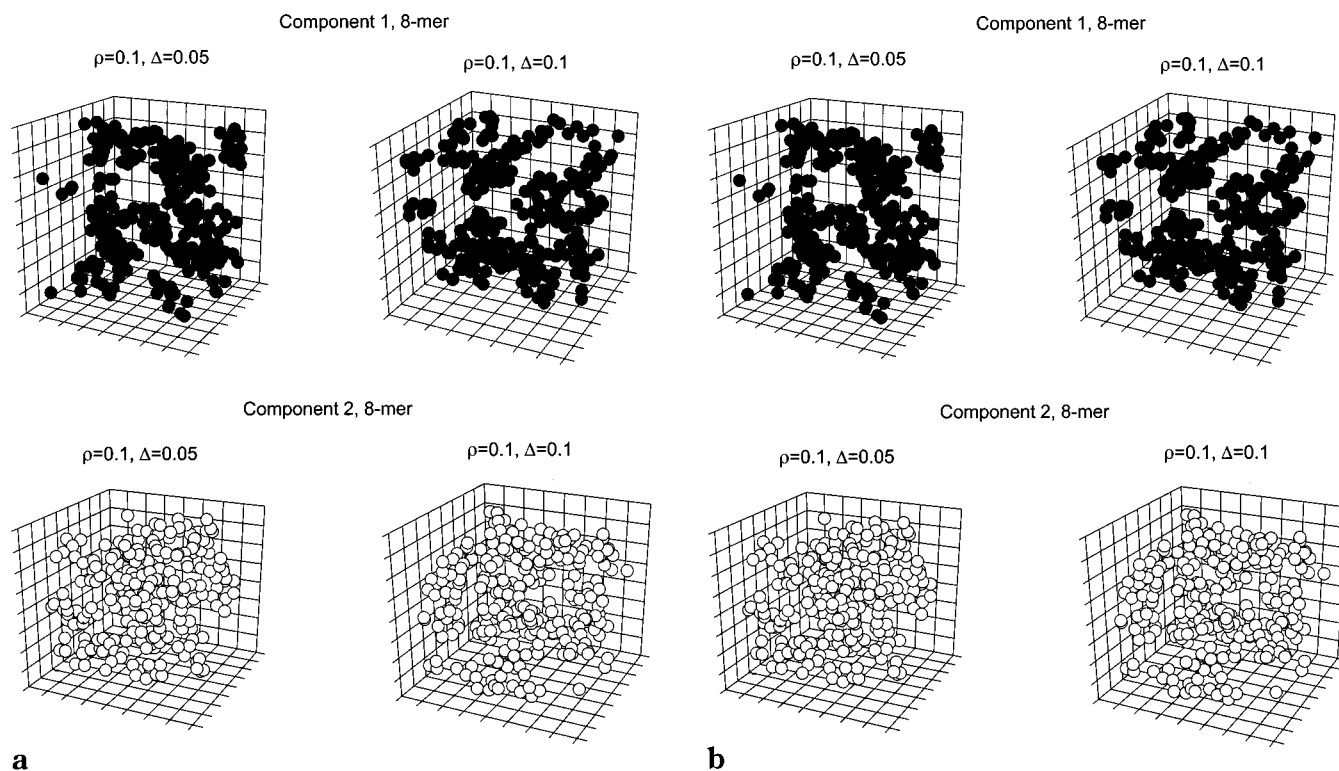


Figure 6. (a) Configuration of the two 8-mer components of the mixture in the simulation box for $\rho = 0.1$ and the two positive $\Delta = 0.05$ and $\Delta = 0.1$. (b) Configuration of the two 8-mer components of the mixture in the simulation box for $\rho = 0.1$ and the two positive $\Delta = 0.05$ and $\Delta = 0.1$.

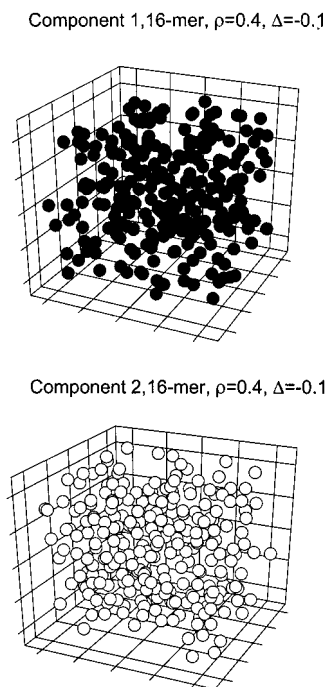


Figure 7. Configuration of the two 16-mer components of the mixture in the simulation box for $\rho = 0.4$ and $\Delta = -0.1$.

component of the mixture at the two positive nonadditivities, while the lower two plots display the second component. Each of the two components is shown in a separate plot with solid and open circles to facilitate visual contrast. It can be easily seen that increasing the density (going from $\rho = 0.1$ to $\rho = 0.4$) leads to an increase in phase separation of the two polymers. The separation is more visible at higher densities and the higher value of Δ . For example, Figure 6b shows that

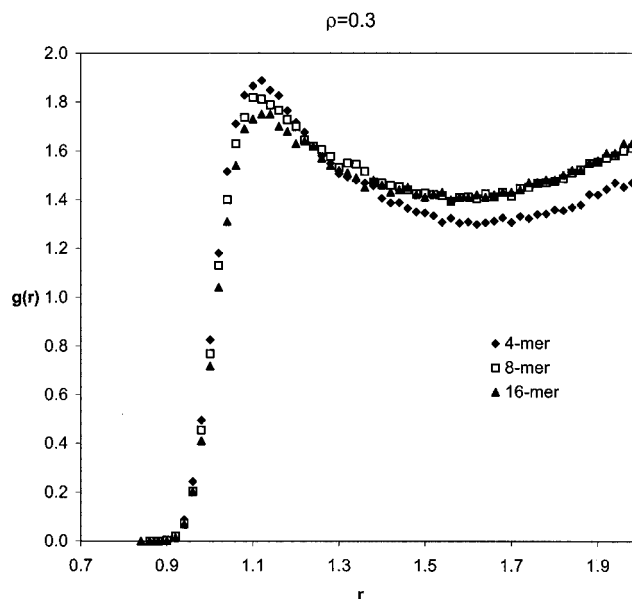


Figure 8. Influence of number of segments per chain on the radial distribution function of segments of the same polymer for $\rho = 0.3$ and $\Delta = 0.05$.

the two components form a layered structure where component 1 aggregates at the center, surrounded by component 2. The same type of behavior is also observed for the 4-mer and 16-mer mixtures. On the other hand, the mixtures are totally miscible at negative and zero nonadditivities and at all densities. An example of a mixture with negative nonadditivity is shown in Figure 7. A good indicator for the level of phase separation is the pair correlation function, g_{ij} . The height of the first correlation peak (g_{ii}) is proportional to the local concentration of the segments of type i around a segment of

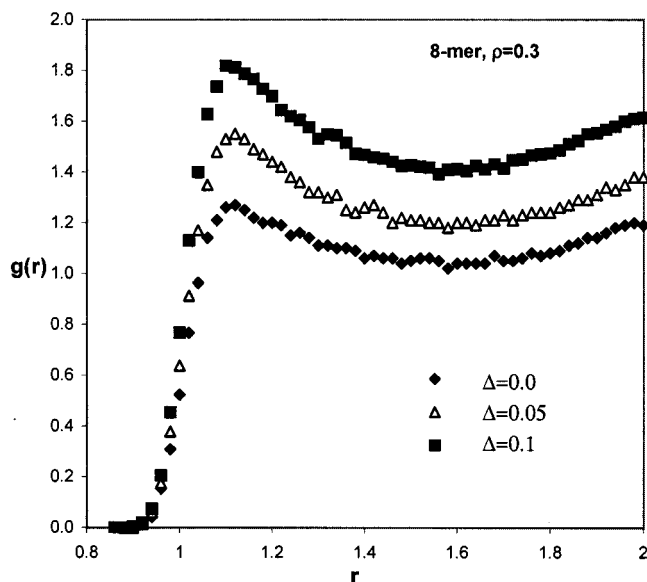


Figure 9. Influence of the magnitude of Δ on the radial distribution function of segments of the same type 8-mer and $\rho = 0.3$.

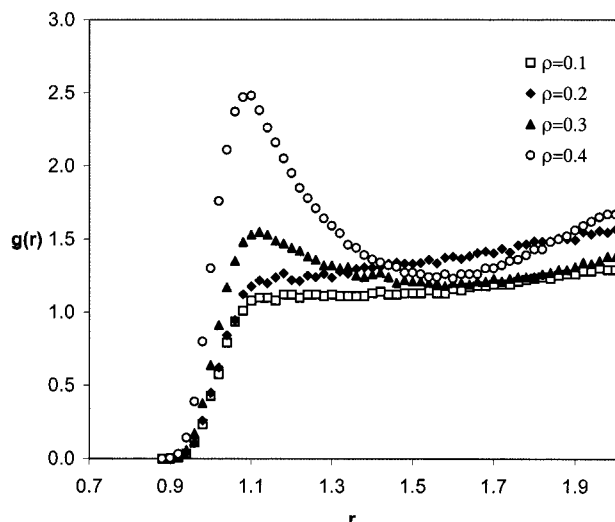


Figure 10. Influence of density on the radial distribution function of segments of the same type 8-mer for $\Delta = 0.05$.

the same type. Figure 8 shows g_{ii} at contact as a function of number of segments per chain at a density of 0.3 and $\Delta = 0.05$. The peak height, which indicates the level of aggregation of the segments of the same polymer, is slightly higher for the shorter chains. This indicates that the shorter chains phase separate more readily at positive Δ because of their higher mobility and their ability to find the equilibrium configuration faster than the longer chains. Figure 9 shows the pair correlation function of the like segments (g_{ii}) at the packing fraction of 0.3 as a function of Δ for the 8-mer. The peak height of the pair correlation function shows a large increase in going from $\Delta = 0.0$ to $\Delta = 0.1$, indicating strong aggregation of the same type polymer segments at positive nonadditivities. Positive nonadditivities with unlike segments have the same effect as repulsions. Consequently, the same type segments aggregate in order to avoid the great repulsions caused by the unlike segments. The aggregation of the same type polymeric segments in distinct domains, resulting in lower repulsions with other constituents of the system, is the main cause of the large negative deviations in compressibility

factor data observed at positive Δ . The higher values of the first correlation peak at higher Δ confirm the visual observations of Figure 6 that exhibit more phase separation at larger Δ . The influence of density on g_{ii} is shown in Figure 10 for $\Delta = 0.05$. A significant increase in the peak value is observed as the density increased, which indicates stronger aggregation of the same component at higher densities.

Further evidence of phase separation in mixtures of nonadditive hard chains can also be investigated graphically by plotting the reduced Helmholtz energy as a function of mol fraction. The reduced Helmholtz energy is calculated by

$$A^* = x_1 \ln(x_1) + x_2 \ln x_2 + \int_0^{\rho} (Z - 1) \frac{d\rho}{\rho} \quad (19)$$

A plot of the Helmholtz energy for mixtures interacting with positive nonadditivity as a function of composition exhibits two minima satisfying the common tangent criterion of material stability and indicating the presence of two stable phases in the system. Minima are absent from systems at low densities and interacting with negative nonadditivities indicating complete miscibility of the two systems at all fractions.

Conclusion

The TPT1 model is found to be more accurate in predicting the compressibility factors for a nonadditive binary mixture of polymers composed of 4, 8, and 16 segments at higher densities and for shorter chains. The PPY model is generally more accurate than the TPT1 model at lower densities and positive nonadditivities. Results of this work show that the two models are valid when nonadditive interactions are present in chain mixtures. The mixture is observed to segregate into distinct phases rich in one of the components when positive nonadditivity is used in the simulation. The phase separation is more apparent at higher densities and larger positive nonadditivity.

Acknowledgment. I would like to thank Dr. W. Smith for providing the DL_POLY program and King Fahd University of Petroleum and Minerals for supporting this research.

References and Notes

- (1) Bates, F. S. *Annu. Rev. Phys. Chem.* **1990**, *41*, 525.
- (2) Helfand, E.; Wasserman, Z. R. *Macromolecules* **1978**, *11*, 960.
- (3) Helfand, E.; Wasserman, Z. R. *Macromolecules* **1980**, *13*, 934.
- (4) Leibler, L. *Macromolecules* **1980**, *13*, 1602.
- (5) Birshtein, T. M.; Skortsov, A. M.; Sariban, A. A. *Macromolecules* **1976**, *9*, 888.
- (6) Dickman, R.; Hall, C. K. *J. Chem. Phys.* **1986**, *85*, 4108.
- (7) Gulati, H. S.; Wichert, J. M.; Hall, C. K. *J. Chem. Phys.* **1996**, *104*, 5220.
- (8) Honnell, K. G.; Hall, C. K.; Dickman, R. *J. Chem. Phys.* **1987**, *87*, 664.
- (9) Fried, H.; Binder, K. *J. Chem. Phys.* **1991**, *94*, 8349.
- (10) Wertheim, M. S. *J. Stat. Phys.* **1984**, *35*, 19. Wertheim, M. S. *J. Stat. Phys.* **1986**, *42*, 477.
- (11) Wertheim, M. S. *J. Chem. Phys.* **1987**, *87*, 7323.
- (12) Chiew, Y. C. *Mol. Phys.* **1990**, *70*, 129.
- (13) Boublik, T.; Vega, C.; Diaz-Pena, M. *J. Chem. Phys.* **1990**, *93*, 730.
- (14) Gazzillo, D. *J. Chem. Phys.* **1991**, *95*, 4565.
- (15) Alblas, P.; van der Marel, C.; Geertsman, W.; Meijer, J. A.; van Osten, A. B.; Dijkstra, J.; Stein, P. C.; van der Lugt, W. *J. Non-Cryst. Solids* **1984**, *61/62*, 201.
- (16) Gazzillo, D.; Pastore, G.; Enzo, S. *J. Phys.: Condens. Matter* **1989**, *1*, 3469. Gazzillo, D.; Pastore, F. R. *J. Phys.: Condens. Matter* **1990**, *2*, 8463.

- (17) Haynes, C. A.; Benitez, F. J.; Blanch, H. W.; Prausnitz, J. M. *AIChE J.* **1993**, *39*, 1539.
- (18) Schouten, J. A.; van den Bergh, L. C.; Trappeniers, N. J. *Chem Phys. Lett.* **1985**, *114*, 40.
- (19) Costantino, M.; Rice, S. F. *J. Phys. Chem.* **1991**, *95*, 9034.
- (20) van Hinsberg, M. G. E.; Verbrugge, R.; Schouten, J. A. *Fluid Phase Equilib.* **1993**, *88*, 115.
- (21) Melnyk, T. W.; Sawford, B. L. *Mol. Phys.* **1975**, *29*, 891.
- (22) Adams, D. J.; McDonald, I. R. *J. Chem. Phys.* **1975**, *63*, 1900.
- (23) Amar, J. *Mol. Phys.* **1989**, *67*, 739.
- (24) Ehrenberg, V.; Schaink, H. M.; Hoheisel, C. *Physica A* **1990**, *169*, 365.
- (25) Jung, J.; Jhon, M. S.; Ree, F. H. *J. Chem Phys.* **1994**, *100*, 9064.
- (26) Jung, J.; Jhon, M. S.; Ree, F. H. *J. Chem Phys.* **1995**, *102*, 1349.
- (27) Tenne, R.; Bergmann, E. *Phys. Rev. A* **1978**, *17*, 2036.
- (28) Schaink, H. M.; Hoheisel, C. *J. Chem. Phys.* **1992**, *97*, 8561.
- (29) Hamad, E. Z. *Mol. Phys.* **1997**, *91*, 371.
- (30) Hamad, E. Z. *J. Chem. Phys.* **1996**, *105*, 3222.
- (31) Hamad, E. Z. *J. Chem. Phys.* **1996**, *105*, 3229.
- (32) Hamad, E. Z. *J. Chem. Phys.* **1997**, *106*, 6116.
- (33) Wilson, M. R.; Allen, M. P. *Mol. Phys.* **1993**, 277.
- (34) Hamad, E. Z. *J. Chem. Phys.*, in press.
- (35) Abu-Sharkh, B. F.; Hamad, E. Z. *Macromolecules* **2000**, *33*, 1345.
- (36) Gao, J.; Weiner, H. J. *J. Chem. Phys.* **1989**, *91*, 3168.
- (37) DL_POLY is a parallel molecular dynamics simulation package written by W. Smith and T. R. Forester at Daresbury Laboratory, Daresbury, Warrington WA4 4AD, U.K.
- (38) Smith, W. S.; Hall, C. K.; Freeman, B. D. *J. Chem. Phys.* **1996**, *104*, 5616.
- (39) Chang, J.; Sandler, S. *Chem. Eng. Sci.* **1994**, *49*, 2777.
- (40) Chapman, W. G.; Jackson, G.; Gubbins, K. E. *Mol. Phys.* **1988**, *65*, 1057.
- (41) Malakhov, A. O.; Brun, E. B. *Macromolecules* **1992**, *25*, 6262.
- (42) Mansoori, G. A.; Carnahan, N. F.; Starling, K. E.; Leland, T. W. *J. Chem. Phys.* **1971**, *54*, 1523.

MA000281V